Mendeleev Communications

Mendeleev Commun., 2026, **36**, 92–94

Synthesis and adsorption properties of Al–Zn and Al–Ni layered double hydroxides

Elizaveta S. Cherepakhina,[a] Daniil A. Logachev,[a] Roman A. Ryabinkin,[a] Anastasia A. Godzishevskaya,[a] Margarita N. Kurasova,[a] Vasili V. Rubanik,[b] Vasili V. Rubanik, Jr.,[b] Victor N. Khrustalev,[a] Anatoly A. Kirichuk,[a] Gunay Z. Mammadova,[c] Abel M. Maharramov[c] and Andreii S. Kritchenkov*[a,b,d]

[a] *Peoples Friendship University of Russia (RUDN University), 117198 Moscow, Russian Federation. E-mail: platinist@mail.ru*
[b] *Institute of Technical Acoustics, National Academy of Sciences of Belarus, 210009 Vitebsk, Republic of Belarus*
[c] *Department of Chemistry, Baku State University, Az 1148 Baku, Republic of Azerbaijan*
[d] *Branch of Petersburg Nuclear Physics Institute named by B. P. Konstantinov of National Research Centre 'Kurchatov Institute' – Institute of Macromolecular Compounds, 199004 St. Petersburg, Russian Federation*

DOI: 10.71267/mencom.7832

Al–Zn and Al–Ni layered double hydroxides were synthesized *via* coprecipitation from solutions of aluminum, zinc and nickel salts at fixed ratios and isolated as polycrystalline samples. The adsorption properties of layered double hydroxides are affected by the nature of the anion in the interlayer space and of the cation in the layers of these compounds.

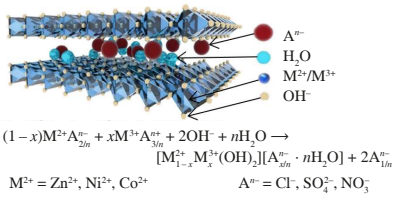

Keywords: layered double hydroxides, adsorption, nickel, zinc, active acid–base sites.

Layered double hydroxides (LDHs) are a class of synthetic and natural inorganic compounds with a complex layered structure and the general formula $[M^{2+}_xM^{3+}_y(OH)_{2x+2y}]^{z+}[A^{n-}_{z/n}\cdot mH_2O]^z$, where M^{2+} and M^{3+} are metal cations forming brucite-like layers, A^{n-} are inorganic or organic anions in the interlayer space and mH_2O represent water molecules of crystallization.[1] LDHs are characterized by a high surface area,[2,3] high adsorption capacity[4,5] and sufficient thermal stability. LDHs are widely used as adsorbents for wastewater treatment,[6,7] catalysts,[8–12] drug delivery systems,[13–15] flame retardants,[16,17] *etc*. Most often, LDHs are employed as sorbents of environmental pollutants, regardless of the size of the sorbed molecule. The interlayer distance in LDHs is not a constant value, this provides the basis for the extremely rich intercalation chemistry of LDHs. Chloride, nitrate, sulfate anions-containing LDHs can be intercalated by replacement of the above anions even by complex bulky organic anions.[18,19] The present work was aimed at the synthesis of Al–Zn and Al–Ni LDHs and the study of their sorption properties with respect to chromate and uranyl ions, which are little available in the publications.

Synthesis of the layered double hydroxides was carried out *via* coprecipitation from solutions of nitrates, sulfates and chlorides of aluminum, zinc and nickel. The molar ratio of divalent to trivalent metal cations (M^{2+} : M^{3+}, where $M^{2+} = Zn^{2+}$, Ni^{2+} and $M^{3+} = Al^{3+}$) was set as 3 : 1 based on the known methods.[20,†] As a result, polycrystalline substances were obtained: white (Al–Zn LDH) and green (Al–Ni LDH) (see Table1).

† Solution A containing a mixture of M^{2+} and M^{3+} salt solutions (C = 0.5 mol dm^{-3}) was added dropwise under constant stirring to solution B, which consisted of an aqueous ammonia solution (C = 1 mol dm^{-3}) and a sodium salt solution with a similar anion (C = 0.1 mol dm^{-3}) in a 12 : 1 ratio. The pH was maintained at ~8–9 throughout the process. The resulting precipitates were aged in the mother liquor at 75 °C for 72 h followed by repeated washing and centrifugation.

X-ray phase analysis of all synthesized samples showed no impurity phases of the starting compounds.[‡] The structure of the obtained materials corresponds to that of the natural mineral hydrotalcite,[21] which confirms the formation of layered double hydroxides. The shift of the first diffraction peak from 2θ = 11° (characteristic of hydrotalcite) to lower angles (9.9° and 10.3°) in samples containing sulfate or nitrate anions indicates an increase in the interlayer distance. When chloride ions are present in the interlayer space, the distance between brucite-like layers decreases, resulting in a peak shift to higher angles (11.4°). Thus, the nature of the anion located in the interlayer space of LDHs significantly affects the structure of these compounds, particularly the interlayer spacing (Figure 1).

In the Fourier-transform infrared (FTIR) LDH spectra, a broad absorption band observed at 3000–3600 cm^{-1} corresponds to O–H stretching vibrations in both brucite-like layers and

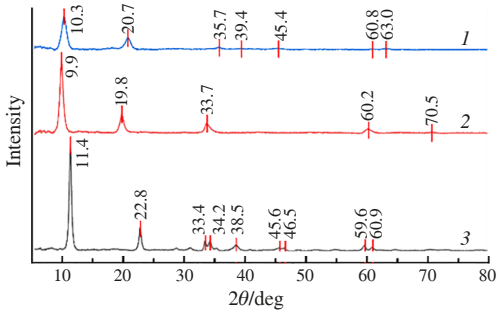

Figure 1 X-ray diffraction pattern of Al–Zn LDH: (*1*) – AZS, (*2*) – AZN, (*3*) – AZC.

‡ X-ray phase analysis was performed using an automatic X-ray diffractometer Tongda TD-3700 for polycrystalline materials in step-scan mode, 2θ range from 5° to 80°, Cu Kα radiation.

© 2026 Mendeleev Communications

interlayer water molecules.[§] The absorption band at 1600–1650 cm^{-1}, attributed to H–O–H bending vibrations, confirms the presence of water molecules in the interlayer space. The spectra show characteristic absorption bands of nitrate anions at 1340 cm^{-1} (N–O stretching vibrations of NO_3^- groups) and 560 cm^{-1} (weak out-of-plane deformation vibrations of NO_3^-). The presence of sulfate anions is evidenced by absorption bands at 1000–1150 cm^{-1} and 580 cm^{-1}, corresponding to S–O stretching vibrations of SO_4^{2-} groups. Metal–oxygen vibrations appear in the region below 500 cm^{-1}. However, due to spectral overlap, it was not possible to discern individual absorption bands corresponding to specific metal–oxygen bonds (M–O, where M = Zn, Ni, Al).

The thermal decomposition process[¶] exhibited gradual dehydration manifested by stepwise mass loss (Figure 2). The first stage (100–300 °C) corresponded to the removal of adsorbed water. The second stage (300–500 °C) involved decomposition of the LDH hydroxide matrix (Table 1). The final thermal decomposition products were identified as a mixture of corresponding oxides.[22] The analysis revealed two distinct mass loss events. The initial endothermic peak between 100–300 °C represents the elimination of physically adsorbed and interlayer water molecules. The subsequent more pronounced mass loss in the 300–500 °C range indicates the decomposition of hydroxyl groups from the brucite-like layers, accompanied by the collapse of the layered structure. The resulting products consist of mixed metal oxides, which is characteristic of LDH thermal decomposition behavior. The observed thermal stability and decomposition pattern are consistent with previously reported data for similar layered double hydroxide systems.[22]

Particle size distribution, which is an important property of the prepared materials, was analysed *via* the dynamic light

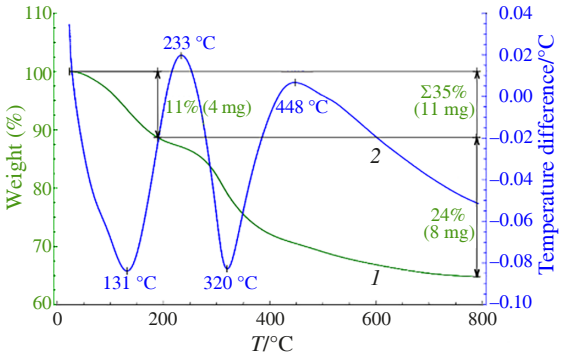

Figure 2 Thermogravimetric (curve *1*) and differential thermal (curve *2*) analysis of Al–Ni LDH Sample (ANC).

Table 1 Results of DTA and TGA.

LDH	T_I/°C	Δm_I (%)	T_{II}/°C	Δm_{II} (%)	$m_{residual}$ (%)
AZN[a]	142	9	253	28	63
AZS[b]	112	18	416	35	47
AZC[c]	143	10	256	27	63
ANN[d]	121	8	339	31	61
ANS[e]	121	11	493	28	61
ANC[f]	131	11	320	24	65

[a] $[Zn_x^{2+}Al_y^{3+}(OH^-)_{2x+2y}]NO_{3\,y/n}^- \cdot zH_2O$; [b] $[Zn_x^{2+}Al_y^{3+}(OH^-)_{2x+2y}]SO_{4\,y/n}^{2-} \cdot zH_2O$; [c] $[Zn_x^{2+}Al_y^{3+}(OH^-)_{2x+2y}]Cl_{y/n}^- \cdot zH_2O$; [d] $[Ni_x^{2+}Al_y^{3+}(OH^-)_{2x+2y}]NO_{3\,y/n}^- \cdot zH_2O$; [e] $[Ni_x^{2+}Al_y^{3+}(OH^-)_{2x+2y}]SO_{4\,y/n}^{2-} \cdot zH_2O$; [f] $[Ni_x^{2+}Al_y^{3+}(OH^-)_{2x+2y}]Cl_{y/n}^- \cdot zH_2O$.

[§] FTIR spectra of the synthesized LDH samples were recorded on an IR-Spirit spectrometer equipped with an ATR (diamond) accessory in the range of 4000–400 cm^{-1}.

[¶] The differential thermal analysis (DTA) and thermogravimetric analysis (TGA) were carried out using a TA Instruments SDT Q600 analyzer with ceramic crucibles. The samples were heated from 30 to 800 °C at the constant heating rate of 10 °C min^{-1}.

scattering method.[††] The analysis showed a bimodal distribution of particles by hydrodynamic radii (565 ± 20 and 832 ± 17 nm for AZN, 61 ± 23 and 719 ± 21 nm for AZS, 610 ± 16 and 883 ± 13 nm for AZC, 489 ± 21 and 697 ± 7 nm for ANN, 588 ± 18 and 955 ± 22 nm for ANS, 394 ± 14 and 780 ± 10 nm for ANC).

The study of CrO_4^{2-} and UO_2^{2+} adsorption was conducted using spectrophotometric method.[‡‡] Adsorption (Q) was calculated using equation:

$$Q = [(C_{initial} - C)V]/m,$$

where $C_{initial}$ is the initial sorbate concentration (mol dm^{-3}), V is the volume of the solution (dm^3), C is the residual (equilibrium) sorbate concentration (mol dm^{-3}) and m is the mass of the sorbent (g). It was shown that the adsorption of CrO_4^{2-} and UO_2^{2+} on the sorbents was fairly active, and the adsorption limit was achieved approximately one day after the start of the experiment (Figure 3). It should be noted that UO_2^{2+} in Al–Ni and Al–Zn systems, same as CrO_4^{2-} in Al–Zn systems, are at the highest rate adsorbed during the first two hours of the experiment. The adsorption of CrO_4^{2-} by Al–Ni systems follows a slightly different pattern, exhibiting relatively uniform absorption during the first day. The most effective sorbents for UO_2^{2+} were ANC and AZC LDH, whereas for CrO_4^{2-}, ANS and AZS were the best sorbents. The observed pseudo-plateau in the range of 60–120 min [Figure 3(*a*)] may indicate a change in the sorption mechanism.[19]

The activity of acidic and basic sites in the LDH samples was evaluated by MO and MB dyes adsorption.[§§] The adsorption results are presented in Figure 4. Based on the obtained data, the most effective adsorption of MO and MB occurs on LDH ANC, ANN and AZC, while the least effective adsorbents are LDH ANS, AZN and AZS. The LDH samples AZN and AZS exhibit almost no basic sites. The activity of acidic sites in the LDH decreases in the series AZC–AZN–AZS and ANC–ANN–ANS, while the activity of basic sites decreases in the series AZC–AZS–AZN and ANN–ANC–ANS. It was found that the studied adsorption is stable: the amount of absorbed dye (both MO and MB) remains practically unchanged after heating the systems at 60 °C for 1 h.

Thus, it was demonstrated that the synthesized layered double hydroxide (LDH) samples have actively adsorbed anions and cations from aqueous solutions. However, the completeness and

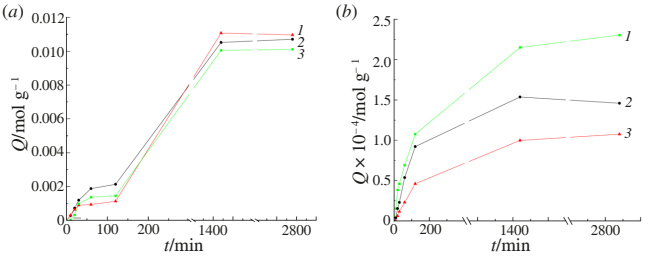

Figure 3 Adsorption curves of (*a*) chromate (CrO_4^{2-}) and (*b*) uranyl (UO_2^{2+}) by Al–Ni LDH: (*1*) – ANS, (*2*) – ANN, (*3*) – ANC.

[††] Photocor Compact-Z particle size analyzer was used at λ = 638 nm and at T = 298 K.

[‡‡] Spectrophotometer SF-103 was used. The concentration of CrO_4^{2-} ions was determined at a wavelength of λ = 410 nm,[23] while UO_2^{2+} – at λ = 430 nm.[24]

[§§] Spectrophotometer SF-103 was used. The concentrations of MO and MB in the test solutions were determined at λ = 465 nm and λ = 665 nm, respectively, selected after obtaining absorption spectra of the initial aqueous dye solutions in the visible range.[25] The stability of dye adsorption was verified for 48 h after the experiment by maintaining the 'LDH–dye solution' systems at 60 °C for 1 h followed by re-measurement of MO and MB content.

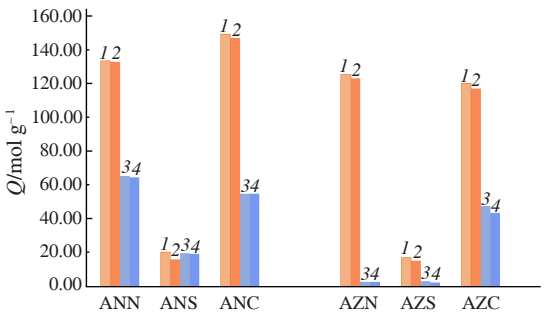

Figure 4 Data on the MO and MB adsorption by Al–Zn and Al–Ni LDH over 48 h: (*1*) – MO, (*2*) – MO after heating, (*3*) – MB, (*4*) – MB after heating.

intensity of adsorption are affected by both the anions present in the LDH interlayer space and the cations forming the brucite-like layers. It is also noteworthy that all LDH samples exhibited high activity of acidic sites, while the basic sites showed particularly high activity in LDHs with chloride anions in the interlayer space.

The study was supported by the grant of the Russian Science Foundation no. 23-23-00022, https://rscf.ru/en/project/23-23-00022/. The authors express their gratitude to the Center for Collective Use 'Physicochemical Research of New Materials, Substances and Catalytic Systems', as well as to Dr. Nikolai Nikolaevich Lobanov for X-ray phase analysis.

References

1 J. Kameliya, A. Verma, P. Dutta, C. Arora, S. Vyas and R. S. Varma, *Inorganics*, 2023, **11**, 121; https://doi.org/10.3390/inorganics11030121.
2 A. A. Sertsova, E. N. Subcheva and E. V. Yurtov, *Russ. J. Inorg. Chem.*, 2015, **60**, 23; https://doi.org/10.1134/S0036023615010167.
3 V. P. Tolstoy, L. B. Gulina and A. A. Meleshko, *Russ. Chem. Rev.*, 2023, **92**, RCR5071; https://doi.org/10.57634/RCR5071.
4 A.-L. Johnston, E. Lester, O. Williams and R. L. Gomes, *J. Environ. Chem. Eng.*, 2021, **9**, 105197; https://doi.org/10.1016/j.jece.2021.105197.
5 R. A. Golubev, A. R. Egorov, N. D. Sikaona, V. E. Esakova, D. I. Semenkova, W. Liu, V. N. Khrustalev, A. A. Kirichuk, A. M. Maharramov, R. H. Nazarov, V. V. Rubanik, V. V. Rubanik, Jr. and A. S. Kritchenkov, *Mendeleev Commun.*, 2025, **35**, 577; https://doi.org/10.71267/mencom.7736.
6 Y. Fu, X. Fu, W. Song, Y. Li, X. Li and L. Yan, *Materials*, 2023, **16**, 5723; https://doi.org/10.3390/ma16165723.
7 S. Sarkar and C. Upadhyay, *Catal. Today*, 2025, **445**, 115101; https://doi.org/10.1016/j.cattod.2024.115101.
8 F. Song and X. Hu, *Nat. Commun.*, 2014, **5**, 4477; https://doi.org/10.1038/ncomms5477.
9 M. Xu and M. Wei, *Adv. Funct. Mater.*, 2018, **28**, 1802943; https://doi.org/10.1002/adfm.201802943.
10 D. S. Bolotin, N. A. Bokach, A. S. Kritchenkov, M. Haukka and V. Y. Kukushkin, *Inorg. Chem.*, 2013, **52**, 6378; https://doi.org/10.1021/ic4000878.
11 A. S. Kritchenkov, N. A. Bokach, G. L. Starova and V. Y. Kukushkin, *Inorg. Chem.*, 2012, **51**, 11971; https://doi.org/10.1021/ic301866y.
12 A. S. Kritchenkov, K. V. Luzyanin, N. A. Bokach, M. L. Kuznetsov, V. V. Gurzhiy and V. Y. Kukushkin, *Organometallics*, 2013, **32**, 1979; https://doi.org/10.1021/om4000665.
13 Ma. F. Peralta, S. N. Mendieta, I. R. Scolari, G. E. Granero and M. E. Crivello, *Sci. Rep.*, 2021, **11**, 20585; https://doi.org/10.1038/s41598-021-00117-9.
14 X. Wang, H. Lu, B. Liao, G. Li and L. Chen, *RSC Adv.*, 2023, **13**, 12059; https://doi.org/10.1039/d3ra01000g.
15 S. Yu, G. Choi and J.-H. Choy, *Nanomaterials*, 2023, **13**, 1102; https://doi.org/10.3390/nano13061102.
16 Y. Gao, J. Wu, Q. Wang, C. A. Wilkie and D. O'Hare, *J. Mater. Chem. A*, 2014, **2**, 10996; https://doi.org/10.1039/c4ta01030b.
17 K. Shanmuganathan and C. J. Ellison, in *Polymer Green Flame Retardants*, eds. C. D. Papaspyrides and P. Kiliaris, Elsevier, Amsterdam, 2014, ch. 2, pp. 675–707; https://doi.org/10.1016/B978-0-444-53808-6.00020-2.
18 A. I. Khan and D. O'Hare, *J. Mater. Chem.*, 2002, **12**, 3191; https://doi.org/10.1039/b204076j.
19 G. R. Williams and D. O'Hare, *J. Mater. Chem.*, 2006, **16**, 3065; https://doi.org/10.1039/b604895a.
20 M. Jobbágy, M. A. Blesa and A. E. Regazzoni, *J. Colloid Interface Sci.*, 2007, **309**, 72; https://doi.org/10.1016/j.jcis.2007.01.010.
21 N. N. Leont'eva, S. V. Cherepanova and V. A. Drozdov, *J. Struct. Chem.*, 2014, **55**, 1326; https://doi.org/10.1134/S0022476614070142.
22 O. V. Nestroinaya, I. G. Ryl'tsova, O. E. Lebedeva, B. M. Uralbekov and O. I. Ponomarenko, *Russ. J. Gen. Chem.*, 2017, **87**, 163; https://doi.org/10.1134/S1070363217020025.
23 L. Xia, E. Akiyama, G. Frankel and R. McCreery, *J. Electrochem. Soc.*, 2000, **147**, 2556; https://doi.org/10.1149/1.1393568.
24 S. A. Kulyukhin and E. P. Krasavina, *Radiochemistry*, 2016, **58**, 405; https://doi.org/10.1134/S1066362216040093.
25 A. P. Tronov, A. V. Tolchev, V. V. Fadeev, V. V. Avdin and R. S. Morozov, *Vestnik YuUrGU. Seriya 'Khimiya' (Bulletin of the South Ural State University. Ser. Chemistry)*, 2024, **16** (4), 154 (in Russian); https://doi.org/10.14529/chem240415.

Received: 26th May 2025; Com. 25/7832